International symposium on Nanostructured, Nanoengineered and Advanced Materials, ISNNAM 2020

Influence of milling parameters on the structural and phase formation in Ti-20%Al alloy through mechanical milling

K.A. Annan[1], P. Daswa[2], K. Motumbo[2] and C.W. Siyasiya[1]

1. Department of Materials Science and Metallurgical Engineering, University of Pretoria, Hatfield, 0002, Pretoria, South Africa
2. Advanced Materials & Engineering (AME), Manufacturing Cluster, CSIR, Meiring Naude Road, Brummeria, 0185, Pretoria, South Africa

E-mail: kofi.annan@up.ac.za

Abstract

Titanium aluminides are considered the choice material for next generation propulsion systems due to their high specific strength and high temperature performance coupled with good oxidation resistance. They are considered best materials for specific applications in the aerospace and automobile industry. Their production process, however, determines the final phase in the alloy, which greatly affects their mechanical properties. The effect of the milling parameters on the particle size and the formation of phases were studied on mechanically alloyed Ti-Al powder. A high-energy ball mill (HEBM) was used to mill a mixture of CP Ti and Al to produce titanium aluminide. The alloy was produced at a fixed ball-to-powder weight ratio of 10:1 whilst varying the milling speed and milling time. The mechanically produced powders were analysed using SEM with EDX and XRD to investigate the chemical homogeneity and the formation of phases after the mechanical alloying technique. The analysis of the mechanically alloyed powders from the mill are reported in terms of the morphology evolution during different milling speed, milling time, elemental composition and the phases formed. Alloys milled at a speed of 500 rpm for a milling time range of 5 to 20 hours revealed the formation of Ti alpha (α-Ti) and gamma phase (γ-TiAl).

Keywords: mechanical alloying; titanium aluminide; TiAl phase*;*

1. Introduction

Titanium aluminide have gained a considerable attention over the last decades due to its high oxidation resistance and strength retention at high temperatures [1-4]. Titanium aluminide is largely used in the manufacturing of high performance gas turbine engines [5] and is primarily considered suitable replacement for Ni based super alloys [6]. At equilibrium conditions, the solubility of Al in Ti is reported to be 0.5% whereas there is no solubility of Ti in Al at room temperature. It has, however, been found that through mechanical alloying process, up to 60 % Al can be dissolved in Ti whilst the solubility of Ti in Al is up to 36 % [7]. The mechanism of phase formation during mechanical alloying is through solid state diffusion process. The identified engineering applicable phases within this alloy are the TiAl or gamma (γ) phase and Ti_3Al or alpha 2 (α_2) phase. The γ is formed between 48.5 and 66 % Al whereas the α_2 is formed between 20 and 39 % Al [7]. A dual phase can be formed between 37 % and 49 % Al. The alpha 2 phase have been identified to exhibit good oxidation resistance and high temperature performance with very little ductility whilst the gamma phase has good oxidation resistance but no ductility at room temperature [8,9]. Research have shown that these problems are somehow resolved with the dual phase but not completely done away with [10-12].

Manufacturing techniques such as casting, forging and rolling which have been traditionally employed to produce the

titanium aluminides are found to be costly with high energy consumption and excessive material loss [13,14]. It has however been pointed out that the above stated difficulties associated with the production process can be overcome through the use of powder metallurgy and the solid state production techniques [15,16]. Mechanical alloying (MA) which is a powder metallurgy process has been identified as a feasible and promising route for cost effective production of Ti based alloys [16-18]. One major problem identified with the MA is the contamination with the milling media and container, which are associated with the processing parameters such as speed, time and ball to powder weight ratio [15]. Mechanical alloying involves repeated deformation, fracturing and re-welding of particles in highly energetic ball collisions [19]. The result is a synthesis of an equilibrium phase with distinct mechanical properties and characteristics, which are dependent on the mechanical milling, process parameters [20]. There is a critical speed at which the balls should be mobilised beyond which the balls get pinned on the walls of the vessel [21]. It is recommended that the rotational speed be set below the critical speed due to the fact that, high speed also increases the milling temperature [16]. This may be advantageous especially if high diffusion and homogenization is a requirement [13] but possible contamination cannot be ruled out in such a situation. On the other hand, increase in temperature may accelerate the transformation process and result in decomposition of metastable phase formed during milling [23]. This paper explores the possibility of producing titanium aluminide with 20 %Al through mechanical alloying by assessing the effect of varying the milling speed and time on the expected alloy phase.

2. Experimental Procedure

The powders used in the current study consist of an 80 wt. % CP Ti and 20 wt. % Al. The ratio of 80% Ti: 20 % Al was chosen in order to increase the ductility of the alloy at room temperature (RT). The Ti was of ASTM grade 2 quality with particle of 100 mesh (~150 µm) whiles the Al was of ASTM grade 1 with particle size of 120 mesh (~120 µm). The starting material comprised of 99.79 % pure Ti and the 99.98% pure Al. The mixture was milled using the Simoloyer high energy ball mill (HEBM), using a high strength stainless steel jar in order to produce a mechanically alloyed Ti20Al alloy powder. The milling speed and milling time were varied as shown in table 1 while ball-to- powder weight ratio (BPWR) was kept constant at 10:1. The mill feed was composed of 200 g powder blend and 2000 g 5 mm diameter 100 Cr6 stainless steel milling balls.

Table 1: Milling speed and time used for the production of Ti20Al alloys.

Milling Parameters	Ti20Al Alloys								
Time (hr)	5	5	5	6	8	14	16	18	20
Speed (rpm)	250	500	1000	500	500	500	500	500	500

Scanning electron microscope (SEM), a JEOL® JSM-instrument 6510 with a tungsten electron gun equipped with energy dispersive –ray spectroscopy (EDX) was used to study the morphology and chemical analysis. X-Ray powder diffraction analysis was carried out in a PAN analytical X-Pert X-Ray diffractometer with Cu Kα radiation (λ = 1.5421 Å). Several powder samples were analysed over the 2θ range of 5 = 90^o with a scanning step size of 2θ = 0.026^o, and a scan rate of 58 seconds/step. X'Pert- High Score® analysis software package was used to analyse the resulting X-ray diffraction patterns.

3.0. Results and Discussion

3.1. Morphology of the as-received Ti and Al elemental powder

The morphology of the as-received Al and Ti elemental powder, and Ti-20 wt. % Al mixture is shown in Figures 1a, 1b and 1c respectively. The particle size distribution of the spheroidized Al powder ranged from 3 to 45 µm, while the irregular Ti powder from 5 to 150 µm.

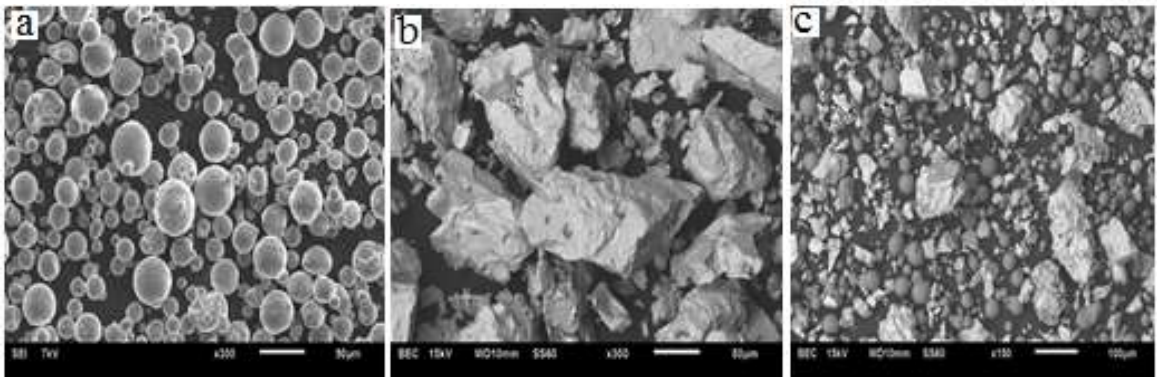

Figure 1: SEM Micrographs of the as received powders showing the morphology of a) Al particles b) Ti particles c) mixture of Ti and Al particles. All images were taken at 300x magnification.

3.2. Effect of milling speed

SEM micrographs of Ti20Al alloys produced at milling speeds of 250, 500 and 1000 rpm are shown in Figures 2a, 2b and 2c respectively. Ti20Al particles change from coarse and irregular shape to fine and flake particles as the milling speed increased.

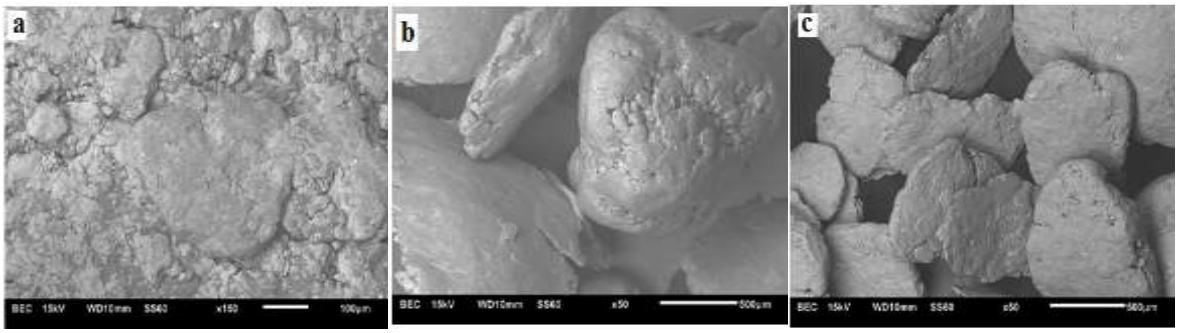

Figure 2: SEM micrographs of Ti+20Al alloys produced at milling time of 5hrs, BPWR of 10:1 and milling speed of a). 250 rpm, b). 500 rpm and c). 1000 rpm. All images were taken at a magnification of 50X

An increase in the homogeneity of the morphology with increasing milling speed was observed as shown by the SEM micrographs in Figures 2. Surface morphology of the alloy produced at 250 rpm was found to be inhomogeneous with individual elements being clearly distinct as seen in the Fig.2a. The 250 rpm sample generally appears to be coarsened and exhibits incomplete alloying. The alloy produced at 500 rpm surface morphology is partially homogeneous. The general appearance of this 500 rpm alloy is finer but shows incomplete alloying with a combination of rounder and flat particles. The alloy produced at 1000 rpm shows a homogeneous surface with finer particles. There appears to be some form of alloying in the sample milled at 1000 rpm but the images are not conclusive enough.

The X-ray diffraction of the mechanically milled Ti20Al alloyed at 250, 500 and 1000 rpm for 5 hours is given in Figure 3. The as mix Ti+20 wt.% Al elemental powder showed a sharp Bragg diffraction peaks of Ti (hcp) and Al (fcc) with high count intensity, and the formation of α-Ti (hcp), γ (TiAl, tetragonal) and Al_3Ti (Tetragonal) stable is revealed.

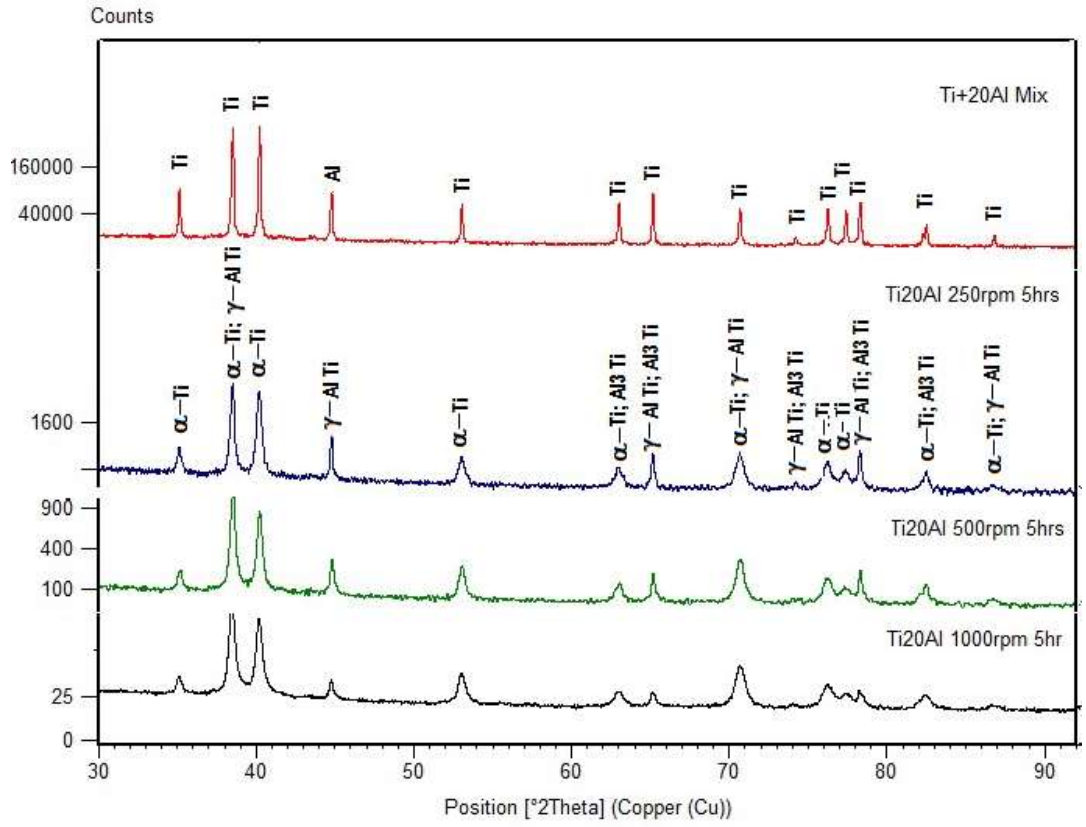

Figure 3: X-ray spectrum of Ti20Al powders milled at different milling speeds

It is worth noting that after milling, Ti and Al peaks had shortened and broadened and some peaks in the range of 60-70 2Θ position completely disappeared with increasing speed. The repeated cold welding and fracturing of particles led initially to solid state reactions/defects enhanced diffusion and subsequently to metastable and stable solid phase transformation (crystalline structure change). This resulted in increase of density of crystalline defects and dislocations. This increased in diffusion resulted in the broadening of the observed XRD peaks [6,7]. Titanium and Aluminium dissolve to form a homogeneous Ti-Al solid solution or phase depending on Ti or Al content [7]. The Ti α-phase, γ-TiAl and Al rich phase such as Al_3Ti are revealed by the XRD analysis. The expected phases in the Ti-Al systems at 80 wt. % Ti and 20 wt.% Al are hexagonal Ti_3Al (α_2) and face-centred tetragonal TiAl (γ), but in the experimental mechanical milling conditions the face-centred tetragonal Al_3Ti was observed instead of Ti_3Al (α_2).

The amount of formed stable phase such as α-Ti (hcp), γ (TiAl, tetragonal) and Al_3Ti (Tetragonal) is given in

Table 2. High content in α-Ti and γ (TiAl) is noticed at milling speed of 500 rpm which is the optimum milling speed of the alloying. Increasing the milling speed decreased the efficiency of the alloying process due to the loss of elemental powder by sticking effect.

Table 2. Phase composition in Ti-20Al mix and alloy after milling for 5 hours at different milling speeds

Elements/Phases, wt.%	*Ti*	*Al*	*α-Ti*	*γ-AlTi*	*Al_3Ti*
Ti-20Al Mix	80	20			
Ti-20Al 250 rpm			78	15	8
Ti20Al 500 rpm	-		69	24	7
Ti20Al 100 rpm	-		89	8	3

The average particle size of Ti20Al alloyed powder plotted as a function of the milling speed is shown in Figure 4. The particles were initially found to be increasing in size due to welding of the particles that took place. The average particle size decreased from about 45 to 20 µm as the milling speed increased from 250 to 1000 rpm. This trend showed a plateau slightly below 45 µm from 1000 rpm for a constant milling time of 5 hours.

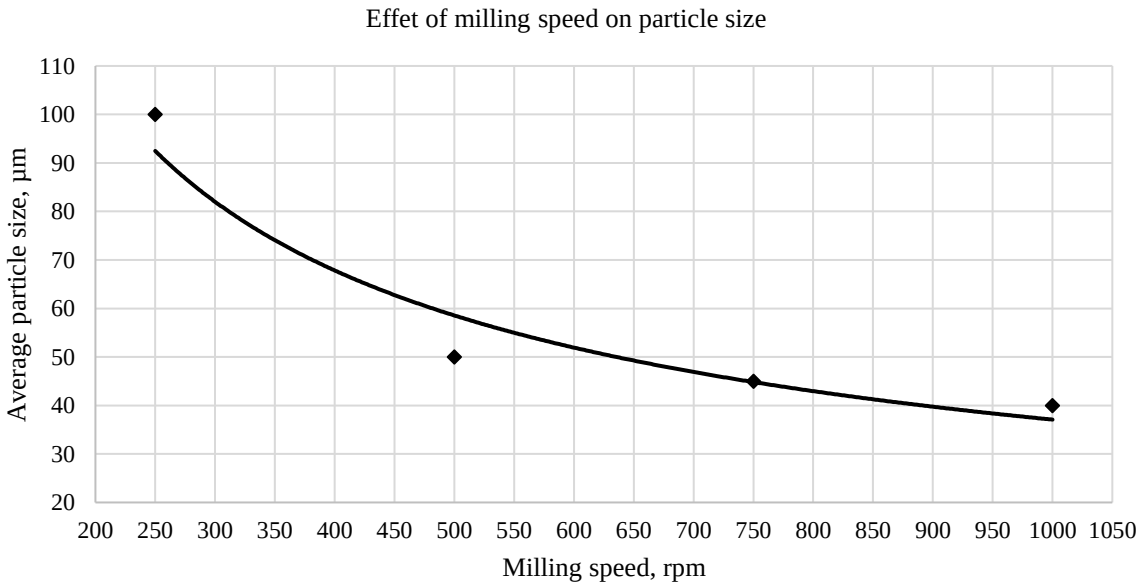

Figure 4: The variation of average particle size of the Ti20Al alloyed powder as a function of the milling speed showing the inverse relationship between the particle sizes and the milling speed.

3.3. Effect of milling time

Figure 5 shows SEM micrographs of the samples milled at different milling times of 6, 10 and 14 hours. The micrographs show that there is an increase in homogeneity with increase in milling time. The morphology of the alloy milled at 6 hours exhibited partial homogeneity consisting of both round and flat shaped particles. The alloy milled at 8 hours have homogenous, rounder, and flat particles whereas the 14 hours milled alloyed being more homogenous and platelet.

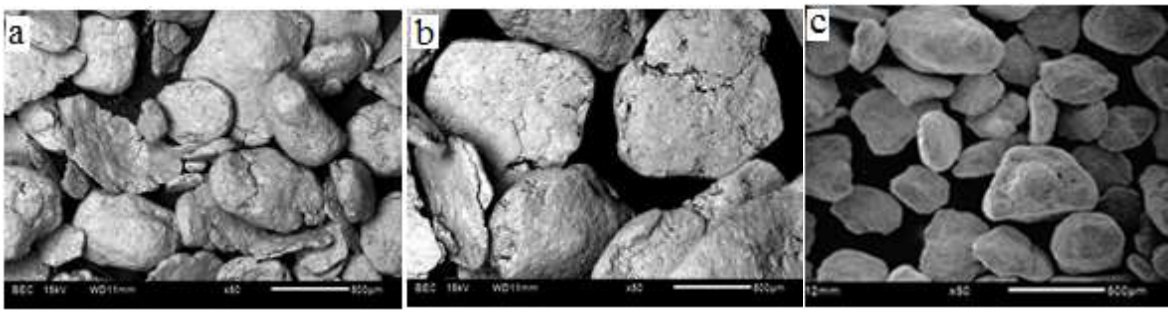

Figure 5: SEM Micrographs of alloys produced at milling speed of 500 rpm, BPR of 10:1 and milling duration of a). 6 hours, b). 8 hours and c). 14 hours. All images taken at a magnification of 50X.

The XRD spectrum of Ti+20Al mixture milled at 500 rpm for 5, 8, 14, 16, 18 and 20 hours is given in Figure 6. The as mix Ti+20 wt.% Al elemental powder showed a sharp Bragg diffraction peaks of Ti (hcp) and Al (fcc) with high count intensity. The formation of α-Ti (hcp), γ (TiAl, tetragonal) and Al_3Ti (Tetragonal) stable is revealed as shown in Figure 6. The XRD patterns displayed a remarkable change as the milling time increased with Ti and Al peaks broadening and decreasing intensity with increasing milling times. The broadening of the peaks signify reduction in crystallite size and inducement of strain in the mechanically alloyed powders. It can generally be noticed that there is an increase in the broadening and the weakening of the peaks of Ti and Al with increased milling time.

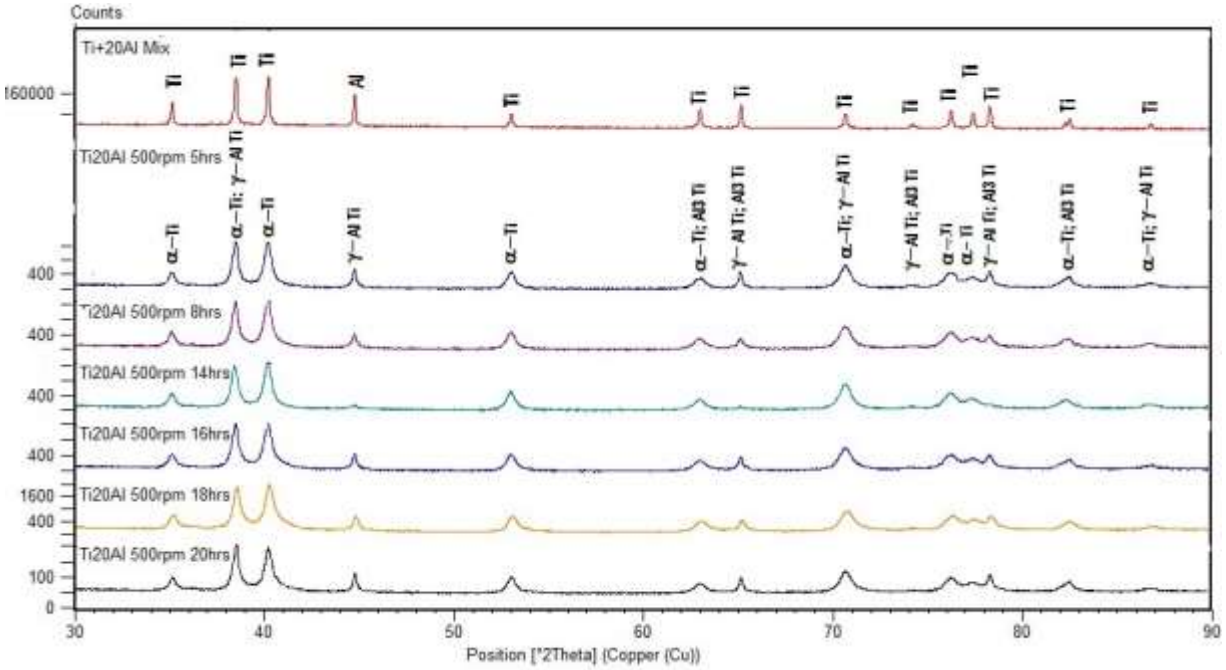

Figure 6: X-ray spectrum of Ti20Al mixture and mechanically alloyed powders milled at different milling times.

The α-Ti (hcp), γ (TiAl, bct) and Al_3Ti (Tetragonal) phase contents are given in Table 3. High content in α-Ti and γ (TiAl) is noticed for milling time of 18 hours. Increasing the milling time had a favourable effect on the alloying process of Ti +20 wt. % Al mixture.

Table 3. Phase composition of Ti-20Al mix and alloy after milling at 500 rpm for different milling times

Elements/Phases, wt.%	*Ti*	*Al*	*α-Ti*	*γ-AlTi*	*Al_3Ti*
Ti-20Al Mix	80	20			
Ti-20Al 5 hrs			69	24	7
Ti20Al 6 hrs	-		77	15	8
Ti20Al 8 hrs	-		79	15	6
Ti20Al 14hrs			79	15	6
Ti20Al 16 hrs			74	19	7
Ti20Al 18 hrs			62	29	9
Ti20Al 20 hrs			72	19	9

A comparison of the principal XRD peaks patterns for different milling times is an indication of an apparent shift for the diffraction peaks to higher angles. The shifting of the peaks shows that the inter-diffusion between different elemental atoms has taken place leading to formation of solid solution of Ti (Al). The line broadening and peak shifting during the mechanical milling at different milling times can be attributed to lowering of lattice parameter of Ti as a result of the Al diffusion which aids in the formation of Ti (Al) through solid solution. This means there is phase formation in the alloy through solid solution during the mechanical alloying process [7]. This solid solution has however proven to be dependent on the milling time during the mechanical alloying process. The broadening of the elemental peaks also confirms a decrease in the effective particle size. Refined Nano particle sizes of TiAl powders were obtained only after 10 hrs of milling time as shown in figure 7.

The average particle size of Ti20Al alloy milled at 500 rpm for 6, 8, 10, 14, 16, 18 and 20 hours is shown in Figure 7. The average particle size decreased from about 45 to 30 nm as the milling time increased from 5 to 20 hours.

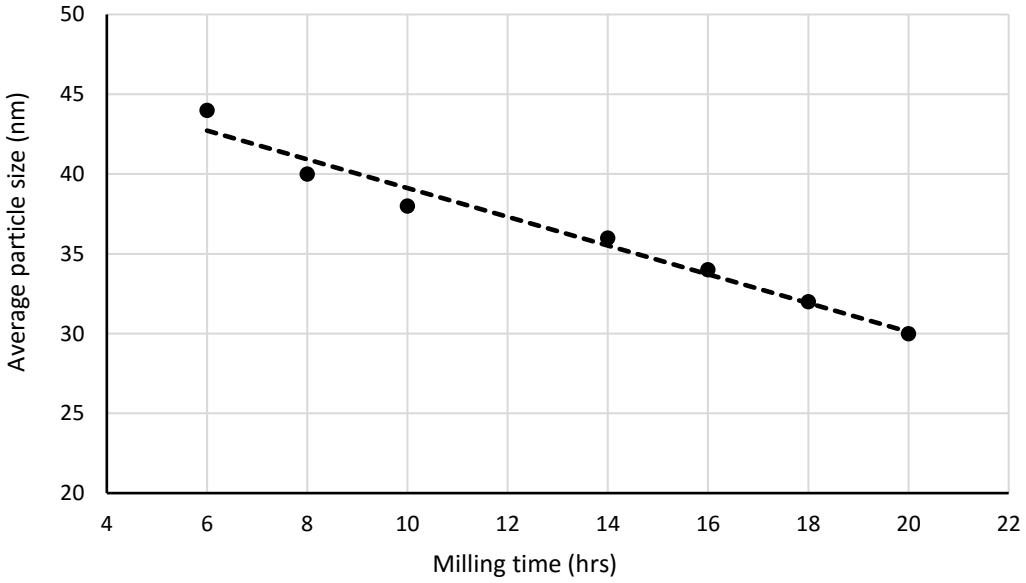

Figure 7: The variation of the average particle size of the Ti20Al alloyed powder as a function of the milling times

3.4. Conclusions

The phase formed, morphology and structure of the Ti-20 wt. % Al powder milled using high speed energy ball mill at varied milling speed and milling times have been investigated. Based on the observations made on the milled alloys at a constant ball to powder ratio of 10:1, the following conclusions were drawn:

- Milling of Ti20Al with Nano crystalline particles sizes has been observed to be formed after 10 hours of milling at a speed of 500 rpm.
- The γ-TiAl (gamma) and α-Ti (alpha) phase content increased with increasing milling time
- Milling Ti+20 wt. %Al mixture led to the formation of α-Ti (hexagonal), Al_3Ti (tetragonal) and γ-TiAl (face-centred tetragonal) stable phases.
- The particle sizes of mechanically alloyed Ti20Al decreased with increasing milling time.

Acknowledgements

The support of the Department of Science and Innovation (DSI) of South Africa, the Council for Scientific and Industrial Research (CSIR) of South Africa and the contribution of the University of Pretoria are dully acknowledged.

References

1. S.M. Soudani, High Performance RX2 Ti 6242S Titanium for Re-useable Launch Vehicles Metallic Thermal Protection Systems, in AIAA Space 2000 Conference & Exposition, AIAA-2000-5147,(2000) 112-120..
2. G. Das, H. Kestler, H. Clemens, and P.A. Bartolotta. Sheet Gamma TiAl: Status and Opportunities, Journal of Materials, (2004) 42-45.
3. S. Djanarthany, J.C. Viala, and J. Bouix. An Overview of Monolithic Titanium Aluminides based on Ti_3Al and TiAl, Materials Chemistry and Physics, vol. 72, (2001) 301–319, 2001.
4. J.P. Immarigeon, R.T. Holt, A.K. Koul, L. Zhao, W. Wallace, and J.C. Beddoes. Lightweight Materials for Aircraft Applications, Materials Charecterization, vol. 34, (1995) 41-67.
5. P. Krause, A. Bartolotta, and L. David. Titanium Aluminide Applications in the High Speed Civil Transport, in International Symposium on Gamma Titanium Aluminides, San Diego, CA, (1999) 1-9.
6. Y.L. Hao, R. Yang, Y.Y. Cui, and D. Li. The Influence of Alloying on the Alpha/(Alpha + Gamma)/Gamma Phase Boundaries in TiAl based Systems, Acta Mater, vol. 48, (2000) 1313-1324.
7. F.W. Bin, X.W. Li, H.F. Sun, and Y.F. Ding. Characterization of Ti-50%Al composite powder synthesized by high energy ball milling. Trans. Non-Ferrors Met.Soc. China, 21. (2011) 333 – 337.
8. K. Bird, and T.A. Wallace. Development of Protective Coatings for High Temperature Metallic Materials, Journal of Space crafts and Rockets, vol. 41, (2004) 213-220.
9. S. Sarkar, S. Datta, S. Das, and D. Basu. Oxidation Protection of GammaTitanium Aluminide using Glass–ceramic Coatings, Surface & Coatings Technology, vol. 203, (2009) 1797–1805.
10. H. Ding, D. Song, D. Wang, C. Zhang, and J. Cui. Microstructural Evolution in Superplastic Deformation of a Ti3Al Alloy," Journal of Material Science Letters, vol. 19, (2000). 1135 – 1137.
11. F. Appel, M. Oehring, J.P.H. Paula, C.H. Klinkenberg, and T. Carneiro. Physical Aspects of Hot-working

Gamma-based Titanium Aluminides, Intermetallics, vol. 12, (2004). 791–802.

12. J. Chraponski, W. Szkliniarz, W. Koscielna, and B. Serek. Microstructure and Chemical Composition of Phases in Ti-48Al-2Cr-2Nb Intermetallic Alloy, Material Chemistry and Physics, vol. 81, (2003) 438-442.
13. H. Hitoshi, Z. and Z. Sun. Fabrication of TiAl Alloys by MA-PDS process and the Mechanical Properties, Intermetallics, vol. 11, (2003) 825-834.
14. X. Lu, X.B. He, B. Zhang, L. Zhang, X.H. Qu, and Z.X. Guo. Microstructure and Mechanical Properties of a Spark Plasma Sintered Ti–45Al–8.5Nb–0.2W– 0.2B–0.1Y Alloy, Intermetallics, vol. 17, (2009). 840–846.
15. M.T Oehring, T. Klassen, and R. Borman. The Formation of Metastable Ti-Al Solid Solutions by Mechanical Alloying and Ball Milling, Journal of Material Research, vol. 8 (11), (2003) 121-129.
16. S. Kumaran, T.R. Srinivasa, R. Subramanian, and P. Angelo. Nanocrystalline and Amorphous Structure Formation in Ti-Al during High Energy Ball Milling," Powder Metallurgy, vol. 48 (4), (2005) 354-358.
17. L Fikeni, KA Annan, M Seerane, K Mutombo, and R Machaka. Development of a biocompatible Ti-Nb alloy for orthopaedic applications, IOP Conference Series: Materials Science and Engineering, vol. 655 (1), (2019) 012-022.
18. P Daswa, Z Gxowa, MJI Monareng, and K Mutombo. Effect of milling speed on the formation of Ti-6Al-4V via mechanical alloying, IOP Conference Series: Materials Science and Engineering, vol. 430 (1), (2018) 012-030
19. R. Tahar, (2015). Characterisation of titanium aluminide alloys synthesized by mechanical alloying technique. PhD Thesis. University Malaysia, Pahang, (2015) 21-24.
20. C. Suryanarayana. Mechanical alloying and milling mechanical engineering, Prog. Mater Sci., Vol. 46, (2001) 175-184.
21. A. Othman, A. Sardarinejad, and A. Masrom. Effect of milling parameters on mechanical alloying of aluminum powders. The International Journal of Advanced Manufacturing Technology, 76(5-8), (2014) 1319-1332.
22. A. Bernatiková, and P. Novák. Structural Changes of TiAl-Based Alloys during Mechanical Alloying. Manufacturing technology conference, Pahang, Malaysia, (2018) 132–139.
23. C. Bettles, S. Tochon, M. Gibson, B. Welk, and H. Fraser. Microstructure and mechanical properties of titanium aluminide compositions containing Fe. Materials Science and Engineering: A, 575, (2013) 152-159.